An Interactive Three Dimensional approach to Anatomical Description – The jaw musculature of the Australian Laughing Kookaburra (*Dacelo novaeguineae*)

The investigation of form-function relationships requires a detailed understanding of anatomical systems. Here we document the 3-dimensional morphology of the cranial musculoskeletal anatomy in the Australian Laughing Kookaburra *Dacelo novaeguineae*, with a focus upon the geometry and attachments of the jaw muscles in this species. The head of a deceased specimen was CT scanned, and an accurate 3D representation of the skull and jaw muscles was generated through manual segmentation of the CT scan images, and augmented by dissection of the specimen. We identified 14 major jaw muscles; 6 in the temporal group (*M. adductor mandibulae* and *M. pseudotemporalis*), 7 in the pterygoid group (*M. pterygoideus dorsalis* and *M. pterygoideus ventralis*), and the single jaw abductor *M. depressor mandibulae*. Previous descriptions of avian jaw musculature are hindered by limited visual representation and inconsistency in the nomenclature. To address these issues, we: (1) present the 3D model produced from the segmentation process as a digital, fully interactive model in the form of an embedded 3D image, which can viewed from any angle, and within which major components can be set as opaque, transparent, or hidden, allowing the anatomy to be visualised as required to provide a detailed understanding of the jaw anatomy; (2) provide a summary of the nomenclature used throughout the avian jaw muscle literature. The approach presented here provides considerable advantages for the documentation and communication of detailed anatomical structures in a wide range of taxa.

1   Michelle R Quayle[1], David G Barnes[2,3,4], Owen L Kaluza[5], Colin R McHenry[1]

3   [1] Department of Anatomy and Developmental Biology, School of Biomedical Sciences, Monash
4   University, Clayton, VIC 3800, Australia
5   [2] Monash Biomedical Imaging, Monash University, Clayton, VIC 3800, Australia
6   [3] VLSCI Life Sciences Computation Centre, Carlton, VIC 3010, Australia
7   [4] Clayton School of Information Technology, Monash University, Clayton, VIC 3800, Australia
8   [5] Monash e-Research Centre, Monash University, Clayton, VIC 3800, Australia

Introduction

The relationship between form and function is a central concept in biology (Lauder et al. 1995; Russell 1916; Thompson 1916); it determines the extent to which the anatomy of an organism permits specific behaviours and ecology. Investigating form-function relationships requires a detailed understanding of anatomical systems, i.e. the discipline of anatomy and morphology. For functional questions concerning feeding ecology, the relevant anatomical system is the feeding apparatus; for the majority of vertebrates, this consists of the jaws. The jaw is a functional unit, consisting of a rigid framework – the skull bones of the cranium and mandible, operated by a system of jaw muscles. The skull bones must be able to withstand the forces of catching a struggling prey item, whilst transferring the bite force generated from the jaw muscles to hold, kill and process the prey without sustaining fracture. Fundamentally, the mechanical limits of the jaw's ability to bite the prey item determines the type and size of prey that can be taken (Ferrara et al. 2011; Herrel et al. 2002; Wroe et al. 2005).

Form-function relationships can be investigated using mechanistic techniques, such as computational biomechanics, and/or quantitative approaches, such as statistics and morphometrics. For biomechanical modelling, the jaw musculature is an important component of the loads that act upon the skull during feeding and other behaviours. During biting, **isotonic** contraction of the adductor musculature imposes reaction forces on the prey (or other item), whilst shaking or twisting of the food requires **isometric** contraction of the jaw muscles to firmly hold the prey. During each of these activities, the activation of the jaw musculature imposes tensile forces to attachment areas which can result in loads at least as high as the loads being applied to the prey (Herring et al. 2001). Therefore, to simulate the jaw as closely to the actual system as possible it is important to include an accurate representation of the jaw musculature in the model.

The following description of the jaw musculature of the Australian laughing kookaburra (*Dacelo novaeguineae*) was stimulated by the need to incorporate detailed anatomical data into high resolution 3D finite element models as part of an analysis of skull biomechanics in 8 species of kingfisher (Alcedines) (Quayle 2011; Quayle et al. in prep.).

43

Avian and kingfisher cranial anatomy

A review of the literature indicates that descriptions of avian jaw anatomy are limited, with
studies of only a few species, use of two-dimensional drawings, and complicated written
descriptions. A major obstacle is the use of differing terminology (Holliday & Witmer 2007).
Papers that incorporate higher levels of detail include Holliday and Witmer's description and
illustration of the albatross jaw musculature (2007), Elzanowski's description of the tinamous jaw
(1987), Zusi and Storer's pied-billed grebe jaw study (1969), Richards and Bock's comparison
of Hawaiian honeycreeper feeding apparatus (1973), and Zweers' description of mallard
myography (1974). From these descriptions it is evident that avian jaw muscle anatomy differs in
relative and absolute size of the various muscles, and in the position and extent of attachments.
Consequently, we determined that the jaw musculature in kingfishers should not be reconstructed
on the basis of anatomical descriptions of other families.

The jaw muscles of several species of kingfisher (though not *Dacelo novaeguineae*) have been
described by Burton (1984); however his illustrations are difficult to interpret, with little
information identifying which part of the skull he is referring to in the figures. Burton's
description did, however, reveal several variations in muscle origin and insertion areas between
the kingfisher species he studied. This observation reinforced the need to document the
kookaburra anatomy independently.

The lack of detailed published data on the kookaburra jaw musculature meant that firsthand
anatomical information was required to accurately model the jaw system. This information was
obtained through the dissection of the head of an adult laughing kookaburra (*Dacelo
novaeguineae*). The kookaburra was CT scanned prior to dissection, and this scan data was used
in conjunction with the dissection information to create a three-dimensional computer model of
the skull and jaw muscles of *D. novaeguineae*.

A 3D approach to anatomical description

Anatomy is inherently three-dimensional, but traditional descriptions of anatomy use a
combination of text and 2D picture modes. New technologies in data collection, assembly,
visualisation and communication, are offering significant new opportunities for improving the
study, documentation and publication of anatomy, particularly given the proliferation of 3D
imaging capabilities.

The following description adopts and exemplifies a three-dimensional approach to displaying
anatomical systems through the use of (1) three-dimensional Adobe Portable Document Format
(3D PDF) figures, and (2) 3D-enabled web pages. The 3D PDF medium allows an interactive 3D
model to be inserted into an electronic document in PDF format, meaning that specialised
software is not required to view the model other than the freely available Adobe Reader (desktop
version), and permanently embedding the figure directly in the document file. This method of
interactive visualisation is becoming increasingly popular, with publications in biomedical

85 science (Kumar et al. 2009; Selvam et al. 2009), astrophysics (Barnes & Fluke 2008),
86 invertebrate (Baeumler et al. 2008; Neusser et al. 2009; Ziegler et al. 2008) and vertebrate
87 anatomy (de Bakker et al. 2012; Holliday et al. 2013; Ruthensteiner & Heß 2008) and
88 paleontology (Knoll et al. 2012; Lautenschlager 2013). In addition, free, open source software
89 that provides a pathway for the generation of 3D PDF figures, especially for use in science, is
90 now available (Barnes et al. 2013).
91
92 The 3D meshes produced for the 3D PDF were also used to generate a model available for
93 viewing in web pages. Web-based 3D visualisation is becoming more common with the growing
94 number of browsers supporting accelerated 2D and 3D graphics, especially via the WebGL
95 standard (http://www.khronos.org/webgl); recent examples include applications in bioinformatics
96 (Pettit & Marioni 2013), neuroinformatics (Ginsburg et al. 2011), and surgical teaching (Birr et
97 al. 2013). Like 3D PDF, web-based 3D visualisation enables the interactive manipulation of a 3D
98 model without requiring specialised software other than a modern web browser.
99
100 Here we present a detailed description of the 3D osteology and jaw musculature of *D.*
101 *novaeguineae,* and provide a summary of the avian jaw muscle synonymies. We aimed to
102 demonstrate and exploit the potential of 3D viewing technology in the anatomical sciences by
103 producing a 3D model that shows the position of the kookaburra jaw muscles on the skull relative
104 to one another; the model can be rotated and superficial muscles hidden or made transparent to
105 allow better visualization of the deeper anatomy. While the 3D model allows for a detailed
106 descriptive model in a single figure-frame, it is only available for viewing in digital format. For
107 this reason, still images suitable for 2D print media are also included.
108
109
110 **Materials & Methods**
111
112 **Specimen**
113 A fresh, deceased adult laughing kookaburra (*Dacelo novaeguineae*), obtained from Australia
114 Museum's Ornithological collection (specimen no. AM BF2162) was used in the following
115 description. This specimen had died in the care of wildlife rescuers as a result of an infection on
116 the right elbow, although the head and skull did not show any obvious pathologies and thus were
117 deemed to illustrate normative anatomy.
118
119 **Data acquisition and processing**
120 The kookaburra was scanned in a clinical computed tomography (CT) scanner (Toshiba Aquilion
121 64) at the Newcastle Calvary Mater Hospital, at 120kV, 75mA and using a slice thickness of
122 0.5mm. The resulting DICOM images were imported into MIMICS v11 (MATERIALISE,
123 Belgium) segmentation software, wherein the skull of the kookaburra was digitally separated
124 from the soft tissue by combining a scalar threshold with manual selection tools; the high density
125 of the bone compared to the surrounding soft tissue allowed for quick and simple segmentation of
126 the skull by applying a threshold based on the grey scale pixel values representative of the bone.

127 A 3D model of the cranium and mandible was then created from this segmentation. This digital
128 skull model provided a scaffold to illustrate the muscle attachment points and muscle geometry
129 determined in the dissection (Fig. 1).
130
131 Segmentation of the jaw muscles proved more difficult due to the small size of the muscles, the
132 low resolution of the scanner and the use of CT (without staining for contrast) rather than MRI.
133 While the soft tissue making up the kookaburra jaw muscles was visible in the CT scan data, and
134 the bellies of the larger muscles could be differentiated and separated using MIMICS
135 segmentation tools, the resolution of the scan was too low to accurately identify the smaller jaw
136 muscles and the muscle attachment sites. For this reason, the soft tissue CT scan data was used
137 alongside the dissection information to identify placement of the jaw muscles (Fig. 1 & Fig. 2).
138
139 The jaw muscles were dissected out beginning with the superficial layer. Each individual muscle
140 was described using drawings, photographs and notes to illustrate its position, direction and
141 attachment sites. Muscles of the hyoid and eye were not required for the biomechanical analysis
142 and were not included in this study. The completed notes on kookaburra muscle anatomy were
143 compared with previously published data on avian jaw musculature (Baumel 1993; Burton 1984;
144 Elzanowski 1987; Holliday & Witmer 2007; Zusi & Storer 1969) to determine the individual
145 names of the jaw muscles observed. Muscle nomenclature used was based on Holliday and
146 Witmer (2007) and Burton (1984). Osteological nomenclature (Fig. 3) was based on Baumel
147 (1993), Zusi and Storer (1969)and Ghetie et al. (1976).
148
149 In conjunction with the CT scan data of the specimen, the illustrated dissection notes were used
150 to digitally recreate a three dimensional representation of the kookaburra jaw musculature on the
151 specimen's skull model (Fig. 2). This model was created using the CT editing software MIMICS
152 to manually select areas of the CT image slices where the muscles were determined to occur. The
153 CT slices were then joined in MIMICS to create a 3D model of each muscle which were
154 individually exported as stereolithography (STL) format files.
155
156 **3D image production**
157 **PDF**
158 A total of 16 segmented surfaces (meshes) – the cranium, mandible, and 14 muscles – comprise
159 the segmented jaw anatomy. The cranium was the largest and most detailed surface, and was
160 remeshed and simplified in MeshLab version 1.3.2 (Visual Computing Lab – ISTI – CNR;
161 http://meshlab.sourceforge.net) using a "Quadric Edge Collapse Decimation" to reduce its facet
162 count from ~635,000 to ~100,000; this reduced the total model size without significant visible
163 degradation. The meshes were converted (using MeshLab) to the widely-used Alias Wavefront
164 ".OBJ" format and listed in a text file, one per line, with colon-separated fields for the part
165 (anatomical) name, a group code, the filename, and the desired part colour expressed as an (r,g,b)
166 triplet. The group code is used to assign parts to named components in a two-level hierarchy. The
167 text file describing the model was read by a small, custom 3D visualization program written
168 using S2PLOT (Barnes et al. 2006), and the surfaces were loaded, coloured and displayed for

169 inspection. Names were applied to the different meshes, and the export capability in the recent
170 S2PLOT release version 3.2.1 (Barnes et al. 2013) was used to save the complete 3-d model to a
171 Product Representation Compact (PRC) format file.
172
173 Additional lines in the model description file were used to: define standard views of the anatomy
174 (left lateral, right lateral, anterior, posterior, dorsal and ventral); to select a basic lighting
175 environment (a headlamp) and background colour; and to define the component group names.
176 From the model description file, a custom views file suitable for PDF embedding was generated,
177 and JavaScript fragments to toggle the various component groups were generated. Following the
178 workflow in Barnes et al. (2013), the PRC model was embedded in a LaTeX-format document
179 (Lamport, *LaTeX: A Document Preparation System (2nd Edition)*, 1994) and compiled into a PDF
180 file with embedded 3D figure, incorporating the custom views file and JavaScript fragments and
181 the standard 3D JavaScript code, included with S2PLOT version 3.2.1, which implements
182 standard keystrokes such as cursor keys to rotate the model and the letter 'a' to toggle autospin
183 mode.
184
185 **Web-based Figure**
186 Our web-based figure is based on the JavaScript *three.js* (http://threejs.org), public domain
187 extensions to *three.js* (via http://learningthreejs.com), and E. Graether's *TrackballControls.js*
188 (http://egraether.com). *Three.js* provides a simple entry point to visualisation of 3D scientific data
189 on the Web by supporting the loading of several common 3D model data formats, and rendering
190 the 3D model using WebGL (http://khronos.org/webgl) where available, and otherwise the 2D
191 Javascript canvas API for devices with no WebGL support. The OBJLoader.js module provides a
192 ready-made importer for the ubiquitous Alias Wavefront OBJ format. Using these components,
193 we developed a custom JavaScript-based web page that reads the identical model description file
194 used for assembling the 3D PDF figure, and constructs a web-based 3D visualisation, coloured as
195 for the 3D PDF version, and offering the same capability to interactively rotate and zoom the
196 model, and to toggle the model components.
197
198
199 **Results**
200
201 **Musculoskeletal anatomy**
202
203 **Depressor Muscles:**
204 1. *M. depressor mandibulae* (mDM) has a fleshy origin on the squamosal region on the back of
205 the braincase, just posterior to the opening of the ear. It becomes thicker as it extends around the
206 jaw joint to insert over most of the posterior surface of the mandible articular bone (Fig. 4 g,h).
207
208 **Temporal Muscles:**
209 The external adductor complex – *M. adductor mandibulae externus* (mAME) – has three parts:
210

211   2. M. *adductor mandibulae externus profundus* (mAMEp) originates along the length of the
212   temporal fossa; the attachment extends from the sagittal midline of the cranium (Fig. 4 g,h,) to
213   the region just dorsal to the zygomatic process and along the posterior edge of the post orbital
214   process. *M. adductor mandibulae externus profundus* inserts onto the coronoid process of the
215   mandible posterior to the insertion of *M. pseudotemporalis superficialis* (Fig. 4 a,b,j).
216
217   3. *M. adductor mandibulae externus superficialis* (mAMEs) has a narrow origin located on the
218   lateral side of the zygomatic process. It extends down around the medial side of the jugal where it
219   fans out to insert widely and thinly over the dorso-lateral surface of the mandibular ramus (Fig. 4
220   a,b,j).
221
222   4. *M. adductor mandibulae externus rostralis temporalis post-orbital lobe* (mAMErt): This
223   muscle is thought to be a member of the adductor mandibulae externus group. Burton (Burton
224   1984) labels it '*M. adductor mandibulae externus rostralis post-orbital slip*' or '*lobe*' in his
225   illustrations but only briefly mentions it in the text. We can find no other literature that uses this
226   term, but we retain its use here in lieu of further information on its possible homology. This
227   muscle was found to have a fleshy origin on the anterior/medial side of the post-orbital process. It
228   inserts onto the coronid process of the manidble, anterior to the insertion of *M. adductor*
229   *mandibulae externus profundus* (Fig. 4 a,b,j). It is clearly separate to the other parts of the
230   external adductor complex (mAME).
231
232   5. *M. adductor mandibulae posterior* (mAMP) originates along the orbital process of the
233   quadrate and the quadrate body (Fig. 4 a,c,i,j). It inserts onto the dorsal side of the mandible,
234   immediately antero-medial to the jaw joint.
235
236   **Pseudotemporalis (mPST) Muscles:**
237   6. *M. pseudotemporalis superficialis* (mPSTs) has two sections (displayed here as one muscle).
238   The medial part originates on the laterosphenoid process on the posterior wall of the orbit (Fig. 4
239   a,c,i). The lateral part originates slightly higher in the depression lateral to the process. Both
240   sections insert onto the medial side of the mandible where they fan out to cover most of medial
241   fossa of the mandible, dorsal to the insertion of M. *pseudotemporalis profundus* (Fig. 4 i,j).
242
243   7. *M. pseudotemporalis profundus* (mPSTp) originates from the medial point of the quadrate
244   orbital process (Fig. 4, a, i). The medial section of the muscle is thick and fleshy, while that
245   lateral side consists of a thin sheet fanning out as it inserts over a large area on the ventral edge of
246   the medial fossa of the mandible (Figure 4 i, j).
247
248   **Pterygoid (PT) Muscles:**
249   8. *M. pterygoideus dorsalis medialis anterior* (mPTDma) originates along the entire length of the
250   medial ridge of the palatine and onto the lateral edge of the pterygoid bone. It inserts onto the
251   anterior end of the mandible's medial process (Fig. 4 d,e,f,n,).
252

253   9. *M. pterygoideus dorsalis medialis posterior* (mPTDmp) takes its origin along the medial side
254   of the pterygoid bone, beginning from the joint of the palatine and pterygoid and inserting onto
255   the anterior edge of the medial mandibular process (Fig. 4 d,e,n).

256

257   10. *M. pterygoideus dorsalis lateralis* (mPTDl) has a fleshy origin on the anterior-most portion of
258   the palatine and down onto the dorsal lateral surface of the palatine. This large muscle wraps
259   down and around to insert onto the ventral/medial side of the mandible (Fig. 4 d,e,f,k,m,n).

260

261   11. *M. pterygoideus ventralis medialis* (mPTVm) originates along the entire ventral surface of the
262   palatine. It extends over the ventral side of the pterygoid bone to insert onto the anterior surface
263   of the tip of the medial mandibular process (Figure 4 k,l,m).

264

265   The *M. pterygoidus ventralis lateralis* (mPTVl) muscle is formed from three parts:

266

267   12. *M. pterygoideus ventralis lateralis Part 1* (mPTVl pt1) is a large, flat, superficial muscle
268   lying most ventral to all others. It originates along the lateral ventral ridge of the palatine and
269   along the lateral side of the crest where the palatine meets the vomer by an aponeurotic sheet
270   extending anteriorly until it merges with the skin of the palate. Posteriorly this muscle becomes
271   thicker as it extends over the posterior end of the mandible to wrap around and insert onto the
272   lateral side of the mandible, posterior to the attachment of *M. adductor mandibulae externus*
273   *superficialis* (Fig. 4 a,b,j,k,l).

274

275   13. *M. pterygoideus ventralis lateralis Part 2* (mPTVl pt2) – this muscle and *M. pterygoideus*
276   *ventralis lateralis part 3* occur closely together and it is possible that they are different heads of
277   the same muscle. Part 2 attaches to the lateral point of the palatine. It then extends back to fan out
278   and attach over a reasonably large area on the ventral side of the entire medial mandibular
279   process (Fig. 4 k,l,m).

280

281   14. *M. pterygoideus ventralis lateralis Part 3* (mPTVl pt3) runs laterally adjacent to Part 2. It
282   originates along the dorsal edge of the palatine, lateral to the palatine attachment of *M.*
283   *pterygoideus dorsalis lateralis.* This muscle attaches to the ventral crest of the medial mandibular
284   process (Fig. 4 f,k,m).

285

286   **3D visualisation**
287   An interactive, 3D model of the jaw muscles described above is available as Figure 5 in the
288   Appendix.

289

290

291   **Discussion**

292

293   **Methodological issues**

294 With the increasing use of CT as a primary means of collecting anatomical data for use in 3D
295 modelling, it is important to note the limitations of this imaging modality. Whilst it is possible to
296 collect the data required for the 3D modelling of the bones from CT alone, our experience with
297 the specimen used in this study is that incorporating detailed muscle anatomy into a 3D model
298 requires a combination of CT imaging and dissection. In CT, contrast between bone and soft
299 tissue is high, which maximises the accuracy of segmentation protocols (both automatic
300 algorithms and manual image processing) for segmenting bones. However, in the absence of
301 fixing protocols (eg. iodine potassium iodide – 'Lugol's iodine'), contrast between muscles and
302 other soft tissues is low and it is difficult to identify individual muscle bellies on the basis of CT
303 data alone; both the perimysium and intermuscular septa are inconsistently visible. An additional
304 limitation is the comparatively low resolution of medical CT in imaging small animals; for the
305 scans used in this study, maximum pixel resolution in each slice was 0.337 mm, which is a
306 relatively large proportion of the maximum cranial diameter (44 mm), even for a large kingfisher
307 species such as the kookaburra. Without the opportunity to use dissection to augment the 3D
308 imaging of muscle anatomy we could not have produced the level of anatomical data presented
309 here.
310
311 Whilst small-animal CT scanners (maximum field of view ~100 mm) or micro-CT (~20 mm) can
312 deliver significantly higher resolution than clinical CT, these scanners are not as readily available
313 as clinical CT scanners and we were not able to utilise one at the time of this study. These higher
314 resolution CT scanners also cannot produce images that clearly differentiate muscle bellies
315 without first preparing the specimen with an iodine stain, and require much longer scan times
316 than a clinical CT.
317
318 It is possible that magnetic resonance imaging (MRI) can provide an alternative to dissection by
319 producing high resolution images of the soft tissue, however MRI is not able to image bone well.
320 A specimen can be both CT and MRI scanned and the resulting images co-registered to fit to the
321 same 3D space co-ordinates, so that CT can be used to model the skeletal elements, while MRI
322 can provide muscle detail. At the time of this study an MRI scanner and co-registration code was
323 not available to us.
324
325 **Nomenclature**
326 Determining the correct names of particular muscles identified in the kookaburra based on
327 previous avian jaw anatomy literature was a complicated process. For many taxonomic groups,
328 anatomical descriptions have ranged across decades, languages, and authors; the issues we
329 discovered with respect to non-standard nomenclature are not restricted to kingfishers. Muscle
330 groups, particularly the *M. adductor mandibulae externus* and *M. pterygoideus dorsalis* muscles
331 were separated into several sections in some studies (Burton 1984; Richards & Bock 1973), or
332 treated as a whole in others (Holliday & Witmer 2007). Within this study, questions remain
333 regarding the extent to which some muscle bellies should be regarded as individual muscles, or
334 be considered as a part of a larger muscle. Specifically, is *M. adductor mandibulae externus*
335 *rostralis temporalis post-orbital* lobe part of one of the other *M. adductor mandibulae externus*
336 muscles (with the only reference found of a separate muscle in this area recorded by Burton

337   (1984); and should *M. pterygoideus ventralis lateralis Part 2* and *Part 3* be considered as
338   separate muscles to *M. pterygoideus ventralis lateralis Part 1*?
339
340   Nomenclature used in this study was based mainly on Burton's (1984) study as it includes
341   kingfisher anatomy and uses similar terminology to Baumel's Nomina Anatomica Avium (1993).
342   However, temporal muscle nomenclature was based upon Holliday and Witmer (2007). Baumel
343   (1993) and Burton (1984) each separate *M. adductor mandibulae externus* into three parts of
344   mAME rostralis, mAME ventralis and mAME caudalis, but we found no clear evidence of 5
345   separate heads for this muscle in *D. novaeguineae*. Holliday and Witmer's nomenclature for the
346   external adductor complex was more similar to the anatomy visible in our specimen.
347
348   There is a lack of consistency in the way in which muscle names are written and abbreviated in
349   text of previous literature. In an attempt to develop a standardised format for writing muscle
350   names and abbreviations, we use the following format:
351   1. When writing the muscle name in text, we use an uppercase 'M.' (contraction for
352   Musculus) at the start of the name, following Baumel's Nomina Anatomica Avium (1993).
353   2. When writing the muscle name in full within text, we italicise the name; hence, *M.*
354   *pseudotemporalis superficialis*. The muscle name is more easily distinguished visually
355   from the surrounding text, making the text easier to read.
356   3. When abbreviating the muscle (e.g. for figure labels), we use lower case for the 'm' and
357   upper case for the abbreviation of the muscle name; hence, mPST. This format visually
358   highlights the informative part of the label.
359   4. Parts of the muscle are written in lower case, hence mPSTs and mPSTp. This makes it
360   easier to identify the muscle under discussion, avoiding the potential confusion that can
361   arise between muscles in the external adductor complex if the abbreviation for the part is
362   written in upper case – Holliday and Witmer (2007) use mAMEP and mAMP for the *M.*
363   *adductor mandibulae externus profundus* and the *M. adductor externus posterior*
364   respectively. We abbreviate these muscles as mAMEp and mAMP.
365
366   Table 1 lists the avian jaw muscle nomenclature that we have used in this paper, the respective
367   abbreviations for use in labels, and the synonymies in selected literature. Note that some of these
368   published nomenclatures were presented as anatomical illustrations rather than written
369   descriptions, making it difficult to accurately determine exact muscle synonymy.
370
371   **The role of 3D images in communicating anatomical information**
372   Descriptive anatomy is the foundation for understanding functional anatomy. The recent surge in
373   biomechanical studies of form-function questions in a range of taxa means descriptive anatomy
374   remains as relevant as ever (Holliday et al. 2013). The current emphasis on 3D modelling
375   approaches indicates that anatomical data should be collated and communicated in 3D, as much
376   as is practically possible. It is certainly possible to communicate anatomical information to the
377   level required for 3D models using text or 2D diagrams; the issue is simply that a great deal of
378   text and/or a large number of 2D images are required. Conversely, a single 3D PDF figure or web

visualisation can communicate an equivalent level of information with the user able to interact
with the model to gain finer understanding of structure.

Acknowledgements

The authors would like to thank; Phillip Clausen, Michael Mahony, Stephen Wroe, John Rodger,
Walter Boles, Jaynia Sladek, Australia Museum, Eleanor Cunningham, Newcastle Calvary Mater
Hospital

References

Baeumler N, Haszprunar G, and Ruthensteiner B. 2008. 3D interactive microanatomy of
        Omalogyra atomus (Philippi,1841)(Gastropoda). *Zoosymposia* 1:101–118.
Barnes DG, and Fluke CJ. 2008. Incorporating interactive three-dimensional graphics in
        astronomy research papers. *New Astronomy* 13:599-605.
Barnes DG, Fluke CJ, Bourke PD, and Parry OT. 2006. An Advanced, Three-Dimensional
        Plotting Library for Astronomy. *Publications of the Astronomical Society of Australia*
        23:82-93.
Barnes DG, Vidiassov M, Ruthensteiner B, Fluke CJ, Quayle MR, and McHenry CR. 2013.
        Embedding and Publishing Interactive, 3-Dimensional, Scientific Figures in Portable
        Document Format (PDF) Files. *PloS one* 8:e69446.
Baumel JJ. 1993. Handbook of avian anatomy: Nomina Anatomica Avium. *Publications of the
        Nuttall Ornithological Club*.
Birr S, Monch J, Sommerfeld D, Preim U, and Preim B. 2013. The LiverAnatomyExplorer: A
        WebGL-Based Surgical Teaching Tool. *Computer Graphics and Applications, IEEE*
        33:48-58.
Burton PJK. 1984. Anatomy and evolution of the feeding apparatus in the avian orders
        Coraciiformes and Piciformes. *Bull of the British Museum (Natural History Zoology ser)*
        47.
de Bakker BS, de Jong KH, Hagoort J, Oostra R-J, and Moorman AFM. 2012. Towards a 3-
        dimensional atlas of the developing human embryo: The Amsterdam experience.
        Reproductive Toxicology 34:225-236.
Elzanowski A. 1987. Cranial and eyelid muscles and ligaments of the tinamous (Aves:
        Tinaformes). *Zoologische Jahrbücher Abteilung für Anatomie und Ontogenie der Tiere*
        116:63-118.
Ferrara T, Clausen P, Huber D, McHenry C, Peddemors V, and Wroe S. 2011. Mechanics of
        biting in great white and sandtiger sharks. *Journal of Biomechanics* 44:430-435.
Ghetie V, Chitescu S, Cotofan V, and Hillebrand A. 1976. *Atlas de Anatomie a Pasarilor
        Domestice*: Editura Academiei Republicii Socialiste Romania.
Ginsburg D, Gerhard S, Calle JEC, and Pienaar R. 2011. Realtime Visualization of the
        Connectome in the Browser using WebGL. *Front Neuroinform Conference Abstract: 4th
        INCF Congress of Neuroinformatics*.
Herrel A, O'Reilly J, and Richmond A. 2002. Evolution of bite performance in turtles. *Journal of
        Evolutionary Biology* 15:1083-1094.
Herring SW, Rafferty KL, Liu ZJ, and Marshall CD. 2001. Jaw muscles and the skull in
        mammals: the biomechanics of mastication. *Comparative Biochemistry and Physiology
        Part A: Molecular & Integrative Physiology* 131:207-219.

428 Holliday CM, Tsai HP, Skiljan RJ, George ID, and Pathan S. 2013. A 3D Interactive Model and
429   Atlas of the Jaw Musculature of *Alligator mississippiensis*. *PloS one* 8:e62806.
430 Holliday CM, and Witmer LM. 2007. Archosaur adductor chamber evolution: integration of
431   musculoskeletal and topological criteria in jaw muscle homology. *Journal of Morphology*
432   268:457-484.
433 Knoll F, Witmer LM, Ortega F, Ridgely RC, and Schwarz-Wings D. 2012. The braincase of the
434   basal sauropod dinosaur *Spinophorosaurus* and 3D reconstructions of the cranial
435   endocast and inner ear. *PloS one* 7:e30060.
436 Kumar P, Vahedi-Faridi A, Saenger W, Merino E, de Castro JAL, Uchanska-Ziegler B, and
437   Ziegler A. 2009. Structural basis for T cell alloreactivity among three HLA-B14 and HLA-
438   B27 antigens. *Journal of Biological Chemistry* 284:29784-29797.
439 Lauder GV, Huey RB, Monson RK, and Jensen RJ. 1995. Systematics and the study of
440   organismal form and function. *BioScience* 45:696-704.
441 Lautenschlager S. 2013. Palaeontology in the third dimension: a comprehensive guide for the
442   integration of three-dimensional content in publications. *Paläontologische Zeitschrift*:1-
443   11.
444 Neusser TP, Heß M, and Schrödl M. 2009. Tiny but complex-interactive 3D visualization of the
445   interstitial acochlidian gastropod *Pseudunela cornuta* (Challis, 1970). *Frontiers in*
446   *zoology* 6:20.
447 Pettit J, and Marioni J. 2013. BioWeb3D: an online webGL 3D data visualisation tool. *BMC*
448   *Bioinformatics* 14:185.
449 Quayle MR. 2011. A Morphological Study of the Kingfisher Skull Environmental Science and
450   Management Honours. University of Newcastle.
451 Richards LP, and Bock WJ. 1973. Functional anatomy and adaptive evolution of the feeding
452   apparatus in the Hawaiian honeycreeper genus *Loxops* (Drepanididae). *Ornithological*
453   *Monographs*:i-173.
454 Russell E. 1916. Form and Function. A Contribution to the History of Animal Morphology. J.
455   Murray. London (Reprint Chicago University Press 1982).
456 Ruthensteiner B, and Heß M. 2008. Embedding 3D models of biological specimens in PDF
457   publications. *Microscopy research and technique* 71:778-786.
458 Selvam L, Vasilyev V, and Wang F. 2009. Methylation of zebularine: a quantum mechanical
459   study incorporating interactive 3D pdf graphs. *The Journal of Physical Chemistry B*
460   113:11496-11504.
461 Thompson DAW. 1916. On Growth and Form. Cambridge University Press.
462 Wroe S, McHenry C, and Thomason J. 2005. Bite club: comparative bite force in big biting
463   mammals and the prediction of predatory behaviour in fossil taxa. *Proceedings of the*
464   *Royal Society B: Biological Sciences* 272:619-625.
465 Ziegler A, Faber C, Mueller S, and Bartolomaeus T. 2008. Systematic comparison and
466   reconstruction of sea urchin (Echinoidea) internal anatomy: a novel approach using
467   magnetic resonance imaging. *BMC Biology* 6:33.
468 Zusi RL, and Storer RW. 1969. Osteology and myology of the head and neck of the pied-billed
469   grebes (Podilymbus). *University of Michigan Miscellaneous Publications of the Museum*
470   *of Zoology* 139:1-49.
471 Zweers GA. 1974. Structure, movement, and myography of the feeding apparatus of the mallard
472   (*Anas platyrhynchos L*.) A study in functional anatomy. *Netherlands Journal of Zoology*
473   24:323-467.
474
475
476
477

Figure 1

Segmentation of the CT data

The CT scan data for the *Dacelo novaeguineae* head was imported into the segmentation software MIMICS (MATERIALISE, Belgium) (a). The skull was segmented out using thresholding tools to select the regions of bone from the scan images, while the muscles were manually segmented. Segmentation is indicated by the coloured regions on the CT image. The segmented regions on each CT image slice were then joined using Mimics modelling tools to create a 3D model of the *D. novaeguineae* skull and jaw muscles (b). The red line through the skull in (b) indicates the location of the CT slice in (a). Jaw muscles shown in this model are 1. *M. depressor mandibulae*, 2. *M. adductor mandibulae externus profundus*, 3. *M. adductor mandibulae externus superficialis*, 4. *M. adductor mandibulae externus rostralis temporalis post-orbital lobe*, 5. *M. adductor mandibulae posterior*, 6. *M. pseudotemporalis superficialis*, 7. *M. pseudotemporalis profundus*, 8. *M. pterygoideus dorsalis medialis anterior*, 9. *M. pterygoideus dorsalis medialis posterior*, 10. *M. pterygoideus dorsalis lateralis*, 11. *M. pterygoideus ventralis medialis*, 12. *M. pterygoideus ventralis lateralis Part 1*, 13. *M. pterygoideus ventralis lateralis Part 2* and 14. *M. pterygoideus ventralis lateralis Part 3*.
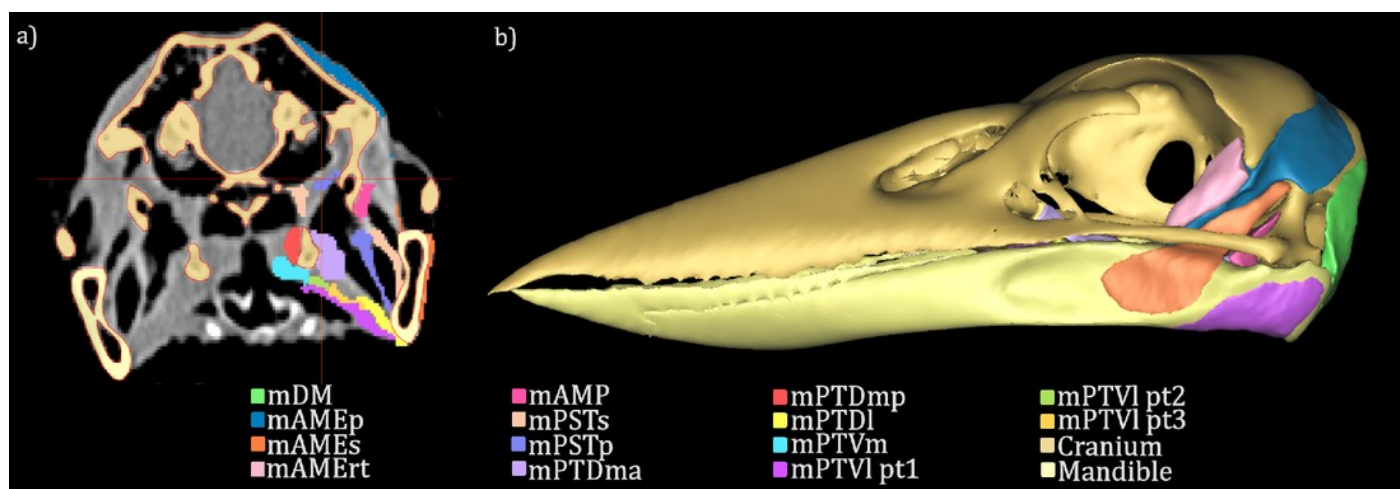
Figure 2

Comparing the dissection to the digital model

Each of the jaw muscles of the laughing kookaburra (*Dacelo novaeguineae*) were individually described and removed during the dissection (a). Notes, drawings and photographs from the dissection were used to identify the jaw muscles on the CT scan so that they could be digitally segmented and modelled (b). This diagram shows the placement of the muscles in the dissected specimen (a) and their digital representation (b). Muscle shown here are 1. *M. depressor mandibulae*, 2. *M. adductor mandibulae externus profundus*, 3. *M. adductor mandibulae externus superficialis*, 4. *M. adductor mandibulae externus rostralis temporalis post-orbital lobe* and 12. *M. pterygoideus ventralis lateralis part 1* (removed in dissection photo).
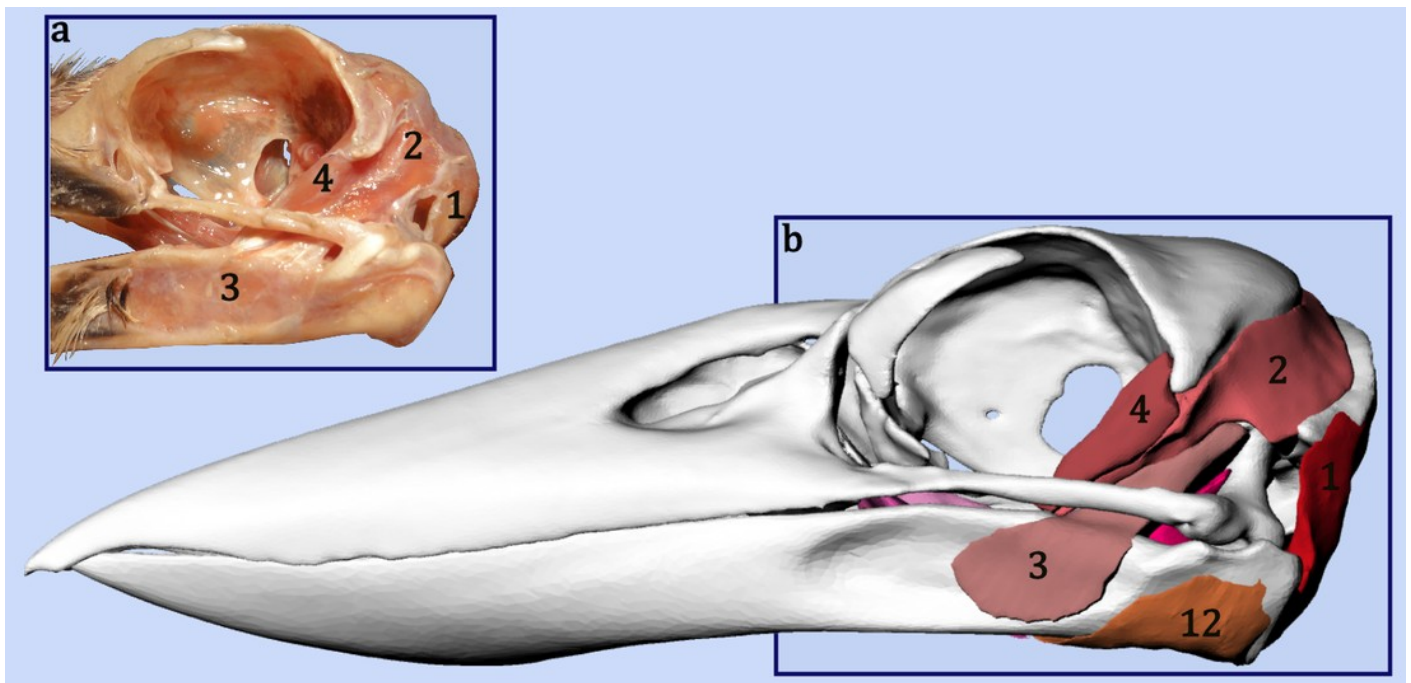
Figure 3

Osteology of the avian skull

Illustrating the bones and features of the avian skull on *Dacelo novaeguineae* in a) anterior, b) posterior, c) lateral, d) dorsal and e) ventral views. f) shows the features of the mandible in dorso-lateral view. Due to the fused nature of avian skull bones, the separation between the bones is not defined. Adapted from (Baumel 1993; Ghetie et al. 1976; Zusi & Storer 1969)
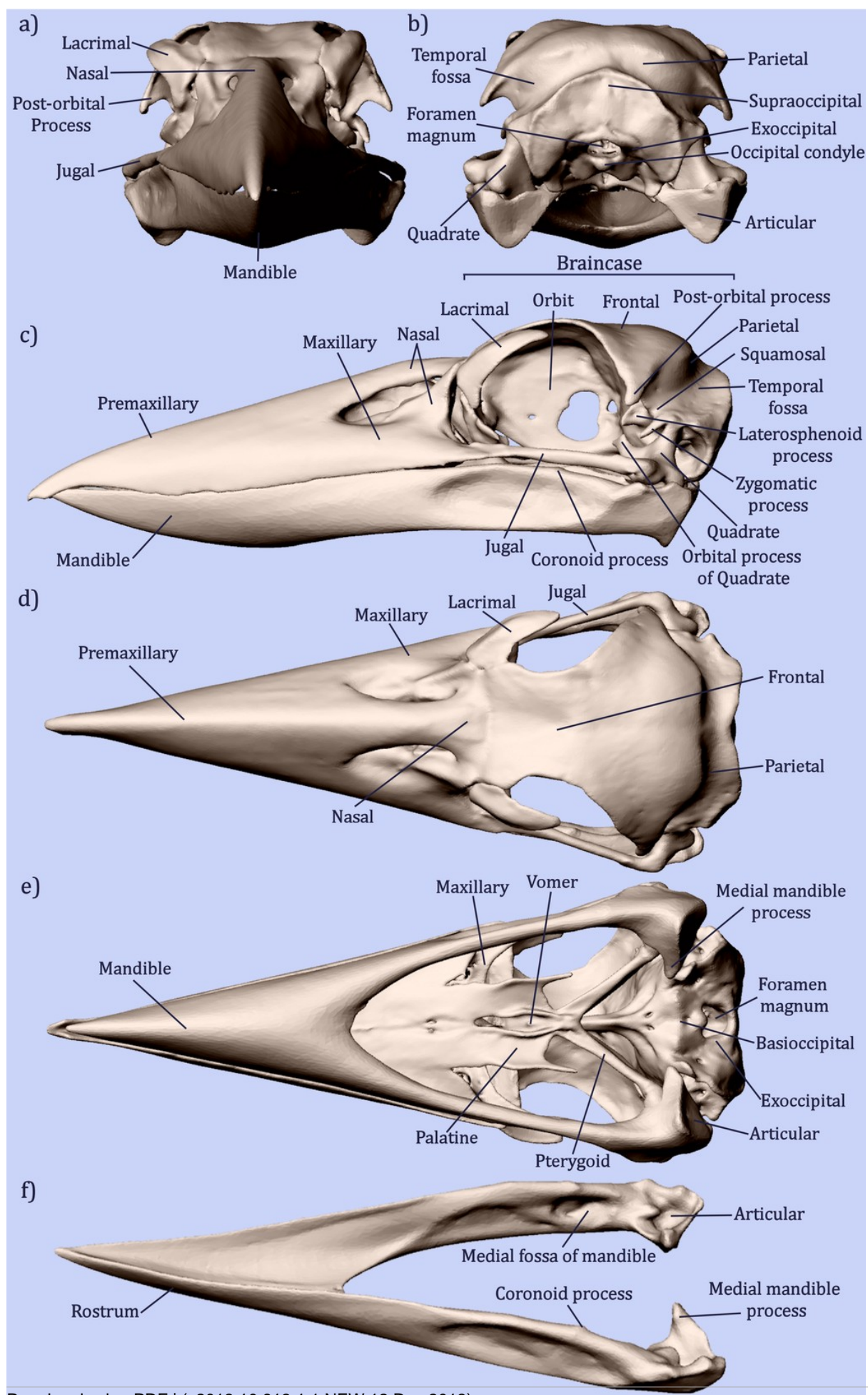
Figure 4

Jaw musculature of the Australian Laughing Kookaburra *Dacelo novaeguineae*

a) Lateral view showing the attachment areas of the jaw muscles, b) the geometry of the jaw muscles and c) deeper muscle geometry with muscle 2,3 and 4 hidden. d) Showing the geometry of the *M. pterygoideus dorsalis* muscles and e) their position in a transparent skull. f) Dorsal view of a transparent skull showing attachment sites of the *M. pterygoideus* muscles to the dorsal side of the palatine and pterygoid bones. g) Attachment sites of muscles on the posterior side of the skull and h) their geometry. i) geometry of the *M. adductor mandibulae externus* and *M. pseudotemporalis* muscles, skull is shown with a transparent mandible to display their medial attachment to the mandible. j) Dorsolateral view of the muscle attachment sites on the mandible. k) Muscle attachment sites on the ventral side of the skull, and the geometry of l) superficial, m) middle and n)deep layers of ventral muscles. 1. *M. depressor mandibulae*, 2. *M. adductor mandibulae externus profundus*, 3. *M. adductor mandibulae externus superficialis*, 4. *M. adductor mandibulae externus rostralis temporalis post-orbital lobe*, 5. *M. adductor mandibulae posterior*, 6. *M. pseudotemporalis superficialis*, 7. *M. pseudotemporalis profundus*, 8. *M. pterygoideus dorsalis medialis anterior*, 9. *M. pterygoideus dorsalis medialis posterior*, 10. *M. pterygoideus dorsalis lateralis*, 11. *M. pterygoideus ventralis medialis*, 12. *M. pterygoideus ventralis lateralis Part 1*, 13. *M. pterygoideus ventralis lateralis Part 2* and 14. *M. pterygoideus ventralis lateralis Part 3*.
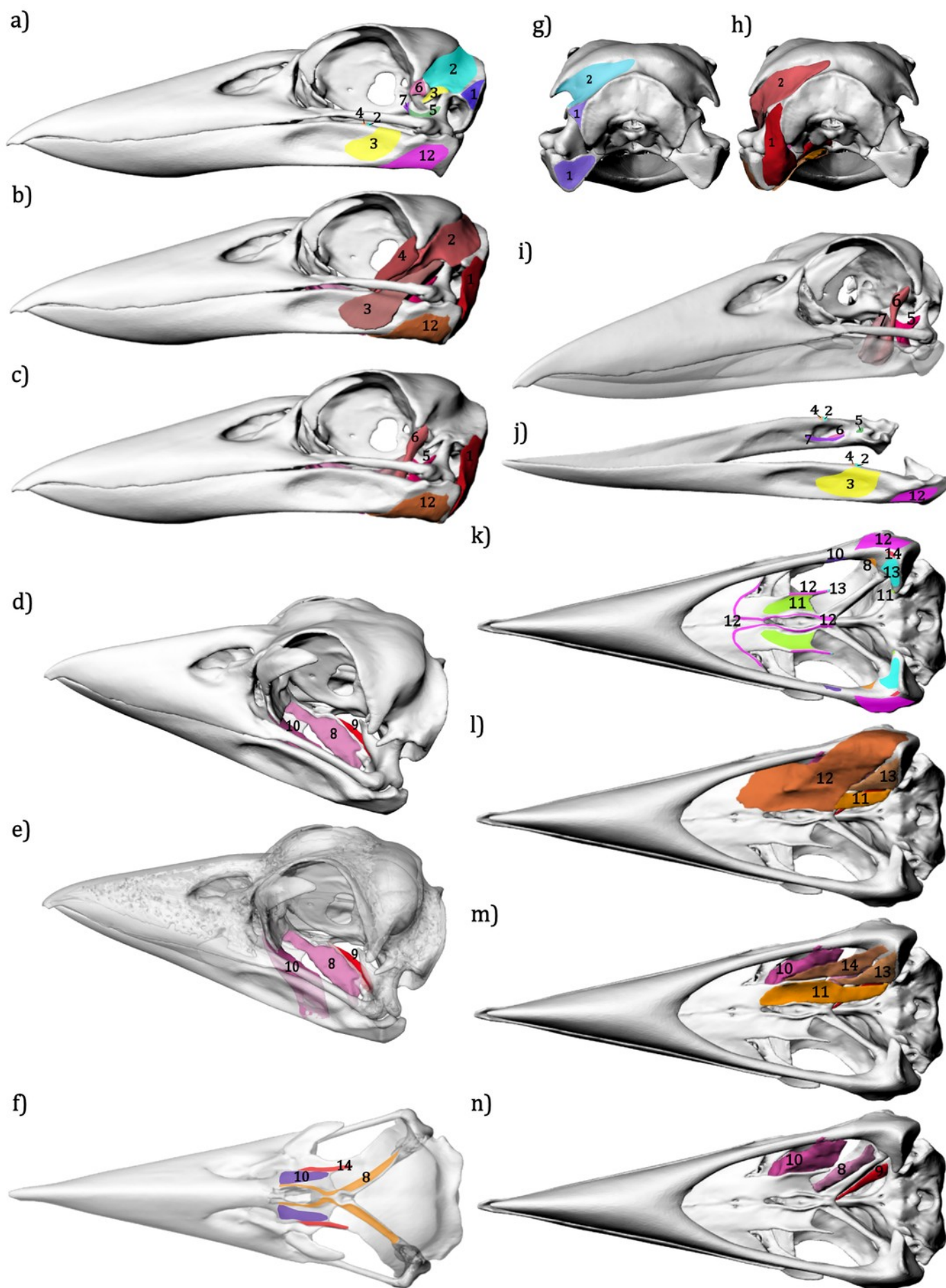
Jaw muscle nomenclature

Equivalent avian jaw muscle names used in this study and selected literature. Muscle equivalents of which we are uncertain are designated by (?).

This study:	This study abbreviation:	Baumel (1993)	Ghetie et al. (1976)	Burton (1984)	Richards & Bock (1973)	Holliday & Witmer (2007)
1. M. depressor mandibulae	mDM	M. depressor mandibulae	M. occipitomandibularis	M. depressor mandibulae	M. depressor mandibulae a,b and c	Not included
2. M. adductor mandibulae externus profundus	mAMEp	M. adductor mandibulae externus rostralis temporalis	M. temporalis	M. adductor mandibulae externus rostralis temporalis	M. adductor mandibulae externus rostralis temporalis	M. adductor mandibulae externus profundus
3. M. adductor mandibulae externus superficialis	mAMEs	M. adductor mandibulae externus rostralis	M. masseter superficialis (?)	M. adductor mandibulae externus rostralis lateralis	M. adductor mandibulae externus rostralis lateralis	M. adductor mandibulae externus superficialis
4. M. adductor mandibulae externus rostralis temporalis post-orbital lobe	mAMErt	Part of M. adductor mandibulae externus rostralis (?)	M. masseter	M. adductor mandibulae externus rostralis temporalis post-orbital lobe	Part of M. adductor mandibulae externus rostralis temporalis (?)	Part of M. pseudotemporalis superficialis or M. adductor mandibulae externus profundus (?)
5. M. adductor mandibulae posterior	mAMP	M. adductor mandibulae externus profundus caudalis	M. quadratomandibularis superficialis	M. adductor mandibulae externus caudalis	M. adductor mandibulae posterior	M. adductor mandibulae posterior
6. M. pseudotemporalis superficialis	mPSTs	M. pseudotemporalis superficialis	M. mandibularis infraorbitalis (?)	M. pseudotemporalis superficialis	M. pseudotemporalis superficialis	M. pseudotemporalis superficialis
7. M. pseudotemporalis profundus	mPSTp	M. pseudotemporalis profundus	M. quadratomandibularis profundus oralis	M. pseudotemporalis profundus	M. pseudotemporalis profundus	M. pseudotemporalis profundus
8. M. pterygoideus dorsalis medialis anterior	mPTDma	M. pterygoideus dorsalis medialis	M. pterygomandibularis (?)	M. pterygoideus dorsalis medialis	M. pterygoideus dorsalis medialis anterior	M. pterygoideus dorsalis
9. M. pterygoideus dorsalis medialis posterior	mPTDmp	M. pterygoideus dorsalis medialis	M. craniopterygoquadratus oralis (?)	M. pterygoideus dorsalis medialis	M. pterygoideus dorsalis medialis posterior	M. pterygoideus dorsalis
10. M.	mPTDl	M.	M.	M.	M.	M.

This study:	This study abbreviation:	Baumel (1993)	Ghetie et al. (1976)	Burton (1984)	Richards & Bock (1973)	Holliday & Witmer (2007)
pterygoideus dorsalis lateralis		pterygoideus dorsalis lateralis	mandibulopalatinus pars lateralis	pterygoideus dorsalis lateralis	pterygoideus dorsalis lateralis	pterygoideus dorsalis
11. M. pterygoideus ventralis medialis	mPTVm	M. pterygoideus ventralis medialis	M. mandibulopalatinus pars medialis	M. pterygoideus ventralis medialis	M. pterygoideus ventralis medialis	M. pterygoideus ventralis
12. M. pterygoideus ventralis lateralis part 1	mPTVl pt1	M. pterygoideus ventralis lateralis	Not determined	M. pterygoideus ventralis lateralis	M. pterygoideus ventralis lateralis	M. pterygoideus ventralis
13. M. pterygoideus ventralis lateralis part 2	mPTVl pt2	M. pterygoideus ventralis lateralis	Part of M. mandibulopalatinus pars medialis (?)	M. pterygoideus ventralis lateralis	M. pterygoideus ventralis medialis fan	M. pterygoideus ventralis
14. M. pterygoideus ventralis lateralis part 3	mPTVl pt3	M. pterygoideus ventralis lateralis	M. entotympanicus (?)	M. pterygoideus ventralis lateralis	Not determined	M. pterygoideus ventralis

3D visualisation of skull bones and jaw musculature in *Dacelo novaeguineae*

This 3D figure is an appendix to Quayle et al., "An Interactive Three Dimensional approach to Anatomical Description - The jaw musculature of the Australian Laughing Kookaburra (*Dacelo novaeguineae*)." If viewing from within Adobe Reader, click on the image to activate the 3D model. To use the model, click to view the label for each structure, left click and drag to free rotate, control left click and drag to pan, use scroll wheel to zoom. Select the "Toggle Model Tree" icon to show/hide individual components of the model. Right click on the component names in the "Model Tree" to make transparent. Muscle labels: 1 mDM *M. depressor mandibulae*, 2 mAMEp *M. adductor mandibulae externus profundus*, 3 mAMEs *M. adductor mandibulae externus supercialis*, 4 mAMErt *M. adductor mandibulae externus rostralis temporalis post-orbital lobe*, 5 mAMP *M. adductor mandibulae posterior*, 6 mPSTs *M. pseudotemporalis supercialis*, 7 mPSTp *M. pseudotemporalis profundus*, 8 mPTDma *M. pterygoideus dorsalis medialis anterior*, 9 mPTDmp *M. pterygoideus dorsalis medialis posterior*, 10 mPTDl *M. pterygoideus dorsalis lateralis*, 11 mPTVm *M. pterygoideus ventralis medialis*, 12 mPTVl pt1 *M. pterygoideus ventralis lateralis Part 1*, 13 mPTVl pt2 *M. pterygoideus ventralis lateralis Part 2* and 14 mPTVl pt3 *M. pterygoideus ventralis lateralis Part 3*.

Figure 5: 3D visualisation of skull bones and jaw musculature in *Dacelo novaeguineae.*
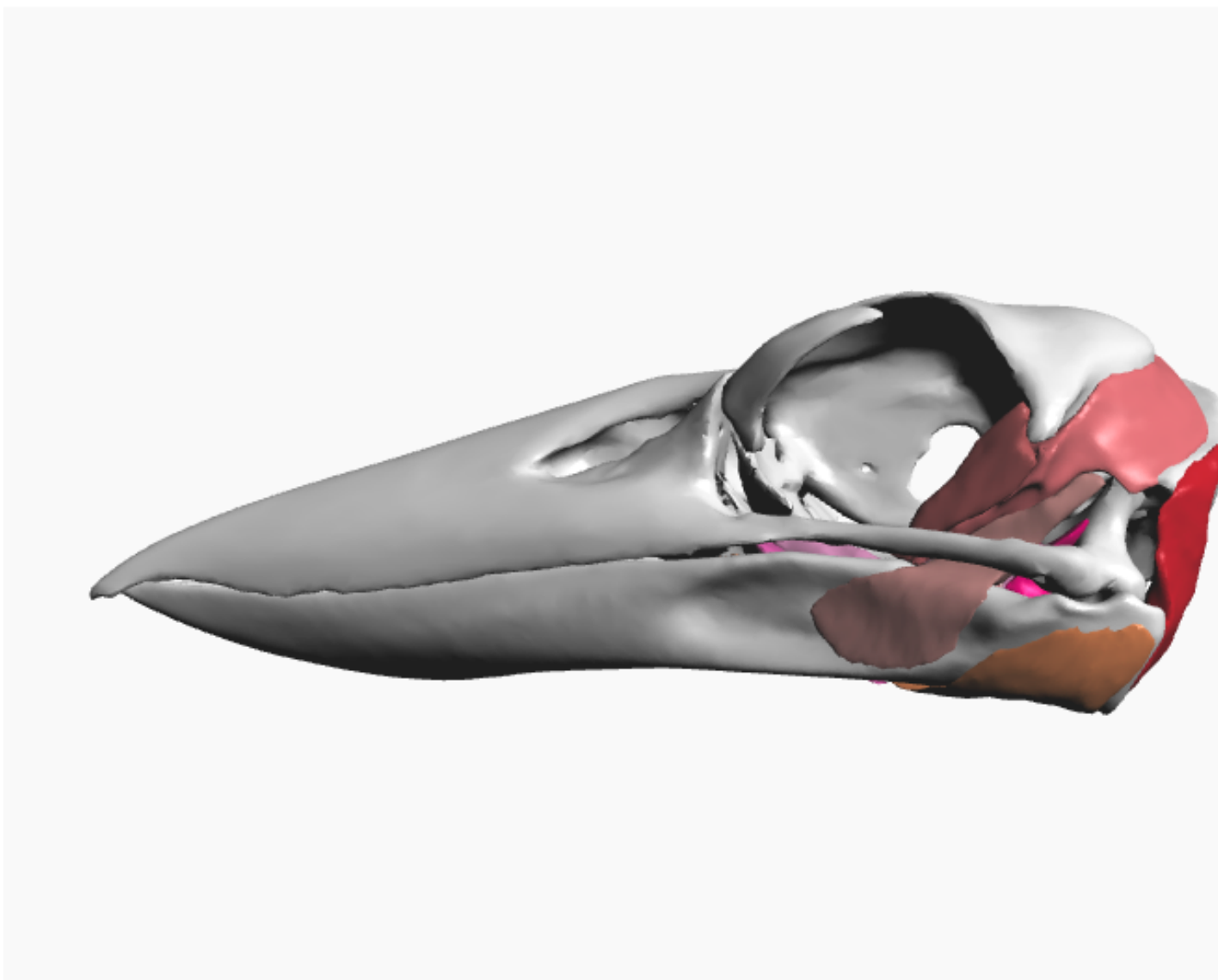
Object:

Toggle: Cranium; Mandible; Depressor muscle; Temporal muscles; Pseudotemporalis muscles; Dorsal Pterygoid muscles; Ventral Pterygoid muscles.

This 3D figure is an appendix to Quayle et al., "An Interactive Three Dimensional approach to Anatomical Description - The jaw musculature of the Australian Laughing Kookaburra (*Dacelo novaeguineae*)." If viewing from within Adobe Reader, click on the image to activate the 3D model. To use the model, click to view the label for each structure, left click and drag to free rotate, control left click and drag to pan, use scroll wheel to zoom. Select the "Toggle Model Tree" icon to show/hide individual components of the model. Right click on the component names in the "Model Tree" to make transparent. Muscle labels: 1 mDM *M. depressor mandibulae*, 2 mAMEp *M. adductor mandibulae externus profundus*, 3 mAMEs *M. adductor mandibulae externus superficialis*, 4 mAMErt *M. adductor mandibulae externus rostralis*, 5 mAMP *M. adductor mandibulae posterior*, 6 mPSTs *M. pseudotemporalis superficialis*, 7 mPSTp *M. pseudotemporalis profundus*, 8 mPTDma *M. pterygoideus dorsalis medialis anterior*, 9 mPTDmp *M. pterygoideus dorsalis medialis posterior*, 10 mPTDl *M. pterygoideus dorsalis lateralis*, 11 mPTVm *M. pterygoideus ventralis medialis*, 12 mPTVl pt1 *M. pterygoideus ventralis lateralis* Part 1, 13 mPTVl pt2 *M. pterygoideus ventralis lateralis* Part 2 and 14 mPTVl pt3 *M. pterygoideus ventralis lateralis* Part 3.